Theor Chim Acta (1995) 90: 383–395

Theoretica Chimica Acta

Calculations of the absorption and emission spectra of p-N,N-dimethylaminobenzonitrile and analogues in solution

Anders Broo, Michael C. Zerner

Quantum Theory Project, Williamson Hall, University of Florida, Gainesville, FL 32611, USA

Received May 18, 1994/Final version received August 25, 1994/Accepted September 16, 1994

Summary. A self-consistent reaction field (SCRF) method that accounts for full electronic relaxation of the initial and final state in an electron transition is derived. The absorption and emission spectra of p-N,N-dimethylaminobenzonitrile (DMABN) and 6-cyanobenzquinuclidine (CBQ) are calculated in different solvents as a test of the method. The results from the fully relaxed SCRF method compare very well with results from a first-order relaxation SCRF model as well as with the experimental absorption and emission spectra of the two molecules considered in detail in this work.

Key words: Absorption spectra – Emission spectra – p-N,N-dimethylaminobenzonitrile – Self-consistent reaction field

In this paper we develop a method to calculate absorption and emission electronic spectra that accounts for full relaxation of the solvent electrons. The method is formulated in a self-consistent reaction field (SCRF) fashion. Recently Karelson and Zerner presented a paper in which the solvent relaxation was treated in a perturbative way [1]. In this paper we will follow the derivation in Ref. 1, but allow the wave function to fully relax in the field created by the electronic transition. The method of full electron relaxation SCRF has previously been used by Broo and Larsson for absorption spectra [2a] and later extended to account for an elliptical cavity shape [2b] and to treat emission spectra [2c]. However, no derivation of the method was given in those works. In the present work four different approaches are considered, in analogy with the work of Karelson and Zerner [1].

Among the most studied emission spectrum is certainly the dual fluorescence found in para-dimethylaminobenzonitrile (DMABN), Fig. 1. Lipert et al. [3] originally observed the phenomenon and assigned the two bands to two different electronic states, one strongly polar (^{1}La) and a second less polar (^{1}Lb). Latter Khalil et al. [4] ascribed the phenomenon to excimer formation in the excited state. A third explanation was put forward by Rotkiewicz et al. [5], in which they assumed that the emission occurred from two different conformers of the excited state, one planar coformer (B*) and one in which the dimethylamino group has

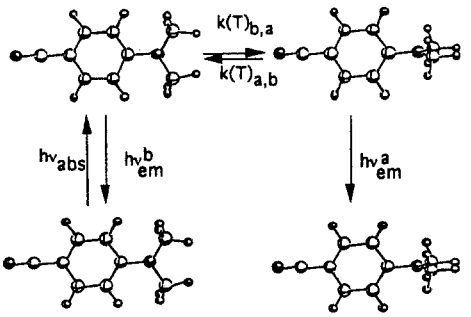

Fig. 1. A possible scheme for the TICT state formation in DMABN. The absorption takes place from the planar conformer (B → B*). The planar excited state can either decay radiatively (k_{f,B^*}) or non radiatively (k_{nr,B^*}) to the ground state or it can undergo a conformation change to the perpendicular conformer. The conformation change is observed to be temperature dependent. The twisted excited state can decay radiatively (k_{f,A^*}) or nonradiatively (k_{nr,A^*})

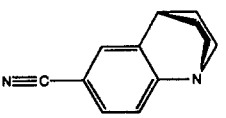

Fig. 2. 6-cyanobezquinuclidine (CBQ)

rotated 90° and is perpendicular to the benzonitrile plane (A*). They described the excited state as a twisted intramolecular charge transfer (TICT) state. The reaction scheme for the TICT model for DMABN is depicted in Fig. 1.

Today the latter explanation is commonly accepted [6] but new alternative explanations of the dual fluorescence of DMABN are still being put forward. In one alternative interpretation of the dual fluorescence of DMABN the N-inversion vibration mode of the dimethylamino group is assumed to decouple the cyano lone-pair from the π-electrons of the phenyl ring [7]. However, neither the results from our work nor the results of a CASSCF/CASPT2 by Roos and coworkers [8] support this alternative explanation without a rotation of the dimethylamino group.

An experimental "proof" for the TICT mechanism was obtained when Rotkiewicz et al. [9] synthesized and characterized the photochemistry of 6-cyano-benzquinuclidine (CBQ). CBQ is an analog compound to DMABN in which the amino group is fixed in an orthogonal conformation with respect to the benzonitrile plane, Fig. 2. The fluorescence spectrum of CBQ has just one broad band at about the same energy as the low energy band (A*) in the fluorescence spectrum of DMABN. The absorption and fluorescence spectra of DMABN and CBQ are calculated as examples of how the fully relaxed SCRF method propose here works.

1. The electronic relaxed self-consistent reaction field method

In the self-consistent reaction field model [10–12] we assume that the solvent can be represented as a structureless continuum. The dielectric properties of the continuum are represented by the static dielectric constant ε and the high-frequency dielectric response, set equal to the refractive index squared, n^2. The solute

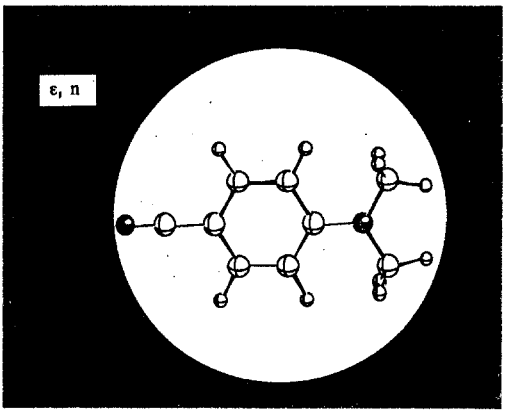

Fig. 3. DMABN in the solvent free cavity used in this work. The shaded area represents the solvent (dielectric) characterized by dielectric ε and index of refraction n

is embedded in a solvent-free cavity. The cavity can be of arbitrary shape but in the work proposed here we consider the case of a sphere with a radius a, see Fig. 3.

Assuming the solute is separated from the solvent by a sphere of radius a, Kirkwood [13] derived a closed expression for the interaction free energy

$$E_{\text{int}} = -1/2 \sum_{l} \sum_{m=-l,1} g_1(\varepsilon) M_{l,m} M_{l,m}, \tag{1}$$

$$g_1(\varepsilon) = (\tfrac{1}{4}\pi\varepsilon_0)\{(l+1)(\varepsilon-1)/[(l+\varepsilon(l+1))a^{(2l+1)}]\}. \tag{2}$$

The second term in the series is the dipole term [14] and is given by

$$E_{\text{int},2} = -\tfrac{1}{2}\{2(\varepsilon-1)/[(2\varepsilon+1)a^3]\}\mu^2 = -\tfrac{1}{2}g(\varepsilon)\mu^2, \tag{3a}$$

$$g(\varepsilon) = g_1(\varepsilon) = g(D') + g(n^2). \tag{3b}$$

Equation (3b) defines D' as the differnce between the equilibrium dielectric constant and the high-frequency dielectric constant.

Although this can be generalized to include higher moments of Eq. (1) [15, 16], we explore only the dipole term here.

Consider an uncharged molecule in solution that absorbs light. We assume that the initial state is in equilibrium with the solvent, and is stabilized by the solvent ($-g(\varepsilon)\mu^2/2$). If we further assume that the absorption or emission process is instantaneous, then only the electron polarization reacts and the final state is destabilized due to the change of charge distribution ($g(n^2)(\mu_i \cdot \mu_i - \mu_i \cdot \mu_f)/2$), where subscript i refers to the initial state and subscript f, to the final state. The absorption or emission process is generally very fast and the solvent nuclei have no time to rearrange in the new charge distribution. This is model A of Ref. [1]. The energies of the initial and final states are given by

$$E_{\text{u},i} = E_i^0 - \tfrac{1}{2}g(D')\langle\psi_i|\mu|\psi_i\rangle \cdot \langle\psi_i|\mu|\psi_i\rangle - \tfrac{1}{2}g(n^2)\langle\psi_i|\mu|\psi_i\rangle \cdot \langle\psi_i|\mu|\psi_i\rangle, \tag{4}$$

$$E_{\text{u},f} = E_f^0 - \tfrac{1}{2}g(D')\langle\psi_f|\mu|\psi_f\rangle \cdot \langle\psi_i|\mu|\psi_i\rangle - \tfrac{1}{2}g(n^2)\langle\psi_f|\mu|\psi_f\rangle \cdot \langle\psi_f|\mu|\psi_f\rangle. \tag{5}$$

The energy difference between the initial and final state is given by

$$\begin{aligned} \Delta E &= E_{\text{u},f} - E_{\text{u},i} \\ &= E_f^0 - E_i^0 - \tfrac{1}{2}g(D')[\langle\psi_f|\mu|\psi_f\rangle \cdot \langle\psi_i|\mu|\psi_i\rangle - \langle\psi_i|\mu|\psi_i\rangle \cdot \langle\psi_i|\mu|\psi_i\rangle] \\ &\quad - \tfrac{1}{2}g(n^2)[\langle\psi_f|\mu|\psi_f\rangle \cdot \langle\psi_f|\mu|\psi_f\rangle - \langle\psi_i|\mu|\psi_i\rangle \cdot \langle\psi_i|\mu|\psi_i\rangle]. \end{aligned} \tag{6}$$

This is the targeted energy difference for either models A or B. As we will discuss below, it is not the only way to view the process of absorption or emission.

Consider the Schrödinger equation of a molecule interacting with an electric field $\boldsymbol{R}$,

$$\boldsymbol{H}|\Psi\rangle = (\boldsymbol{H}^0 - \boldsymbol{\mu}\cdot\boldsymbol{R})|\Psi\rangle \tag{7a}$$

In our case, $\boldsymbol{R}$ is a reaction field as given below:

$$\begin{aligned}\boldsymbol{H}|\Psi\rangle &= [\boldsymbol{H}^0 - g(D')\langle\psi_i|\boldsymbol{\mu}|\psi_i\rangle\cdot\boldsymbol{\mu} - \tfrac{1}{2}g(n^2)[\langle\psi_i|\boldsymbol{\mu}|\psi_i\rangle + \langle\psi_f|\boldsymbol{\mu}|\psi_f\rangle]\cdot\boldsymbol{\mu}]|\Psi\rangle \\ &= W|\Psi\rangle \end{aligned} \tag{7b}$$

with corresponding Fock operator given by

$$f_A(k) = f^0(k) - g(D')\langle\psi_i|\boldsymbol{\mu}|\psi_i\rangle\cdot\boldsymbol{\mu}(k) - \tfrac{1}{2}g(n^2)[\langle\psi_i|\boldsymbol{\mu}|\psi_i\rangle + \langle\psi_f|\boldsymbol{\mu}|\psi_f\rangle]\cdot\boldsymbol{\mu}(k) \tag{8}$$

and the orbital equation

$$f_A(k)|\phi_j(k)\rangle = \varepsilon_j|\phi_j(k)\rangle, \tag{9}$$

The energy difference between initial and final states using these equations is given by

$$\begin{aligned}\Delta E_{\mathrm{qm}} = W_f - W_i &= \langle\Psi_f|\boldsymbol{H}^0|\Psi_f\rangle - \langle\Psi_i|\boldsymbol{H}^0|\Psi_i\rangle \\ &\quad - g(D')[\langle\psi_f|\boldsymbol{\mu}|\psi_f\rangle\cdot\langle\psi_i|\boldsymbol{\mu}|\psi_i\rangle - \langle\psi_i|\boldsymbol{\mu}|\psi_i\rangle\cdot\langle\psi_i|\boldsymbol{\mu}|\psi_i\rangle] \\ &\quad - \tfrac{1}{2}g(n^2)[\langle\psi_f|\boldsymbol{\mu}|\psi_f\rangle\cdot\langle\psi_f|\boldsymbol{\mu}|\psi_f\rangle - \langle\psi_i|\boldsymbol{\mu}|\psi_i\rangle\cdot\langle\psi_i|\boldsymbol{\mu}|\psi_i\rangle]. \end{aligned} \tag{10}$$

ΔE_{qm} is not the original energy difference ΔE. ΔE represents the energy of the solute and the solvent. Equations such as (1)–(6) are derived under the assumption that the wave function is separable into solvent and solute parts. Equation (7) only considers the quantum mechanical part and W therefore represents the energy of the solute and its interaction with the solvent [1]. We must add to ΔE_{qm} the term

$$\Delta E_{\mathrm{solv\ cost}} = -\tfrac{1}{2}g(D')\langle\psi_i|\boldsymbol{\mu}|\psi_i\rangle\cdot[\langle\psi_f|\boldsymbol{\mu}|\psi_f\rangle - \langle\psi_i|\boldsymbol{\mu}|\psi_i\rangle], \tag{11}$$

$$\Delta E = \Delta E_{\mathrm{qm}} + \Delta E_{\mathrm{solv\ cost}}, \tag{12}$$

where $\Delta E_{\mathrm{solv\ cost}}$ may be viewed as the difference in energy between the final and the initial states that the solvent lost in dissolving these two states of the solute.

An alternative way to derive a Fock operator is to require that the total energy of each state be given directly by Eqs. (4) and (5). This leads to a Fock operator given by (model B of Ref. [1]).

$$f_B(k) = f^0(k) - \tfrac{1}{2}g(D')\langle\psi_i|\boldsymbol{\mu}|\psi_i\rangle\cdot\boldsymbol{\mu}(k) - \tfrac{1}{2}g(n^2)[\langle\psi_i|\boldsymbol{\mu}|\psi_i\rangle + \langle\psi_f|\boldsymbol{\mu}|\psi_f\rangle]\cdot\boldsymbol{\mu}(k). \tag{13}$$

With this approach, the energy difference ΔE is obtained directly from the quantum mechanical calculation.

Another way to view the absorption or emission process is to assume that the electrons of the solvent are in equilibrium with those of the solute during the entire absorption (or emission) process. This leads to equations in which both ground and excited state see a "mean" field. The Fock operators for this mean field approach

are then given by (models A1 and B1 of Ref. [1]).

$$f_{A1}(k) = f^0(k) - g(D')\langle\psi_i|\mu|\psi_i\rangle\mu(k) - \tfrac{1}{4}g(n^2)[\langle\psi_i|\mu|\psi_i\rangle + \langle\psi_f|\mu|\psi_f\rangle]\mu(k), \tag{14}$$

$$f_{B1}(k) = f^0(k) - \tfrac{1}{2}g(D')\langle\psi_i|\mu|\psi_i\rangle\mu(k) - \tfrac{1}{4}g(n^2)[\langle\psi_i|\mu|\psi_i\rangle + \langle\psi_f|\mu|\psi_f\rangle]\mu(k). \tag{15}$$

Since the Fock operators, for all four models depend both on the wave function itself and the (dipole) moments of the initial and final states the problem is solved by an iterative scheme.

In our implementation one assumes for the first cycle that the excited state of interest has zero elements, $\langle\psi_f|\mu|\psi_f\rangle = 0$, and uses the SCF ground state dipole moment for $\langle\psi_i|\mu|\psi_i\rangle$. The CI then yields values for $\langle\psi_f|\mu|\psi_f\rangle$ and $\langle\psi_i|\mu|\psi_i\rangle$ which are then used for an SCF-CI cycle. This procedure is considered converged when the change in the ground and excited state dipole moments are less than 10^{-4} Debye. By this criterion the transition energies are converged to within 1 cm^{-1}.

This procedure works on a pair of states, $|\psi_i\rangle$ and $|\psi_f\rangle$, at one time; that is, $|\psi_i\rangle$ and $|\psi_f\rangle$ are coupled. The states obtained in each calculation are orthogonal, $\langle\psi_f^f|\psi_i^f\rangle = 0$, but there is a different $|\psi_i^f\rangle$ for each final state considered. Here the superscript refers to a particular final state used in forming the Hamiltonian, and this orthogonality problem arises as we are using a different Hamiltonian for each pair of states. In practice, $\langle\psi_0^f|\psi_0^{f'}\rangle > 0.99$ for all the cases we have examined. Similarly $\langle\psi_f^f|\psi_{f'}^{f'}\rangle \neq 0$ for $f \neq f'$, but their overlap is generally small. These observations suggest, as we will see in the next section, that the first-order theories A1, etc., yield results that are similar to these results in which the electronic polarization is allowed to completely relax. In these first-order theories a single diagonalization of a CI matrix is corrected for electronic polarization, and all states obtained remain orthonormal.

Equations (8), (13)–(15) yield ΔE directly. They are iterative in nature to do so. A simpler model uses the Fock operator [1]

$$f_A(k) = F_A^0(k) - g(\varepsilon)\langle\psi_i|\mu|\psi_i\rangle\mu(k) \tag{16}$$

or

$$f_B(k) = F_B^0(k) - g(\varepsilon)\langle\psi_i|\mu|\psi_i\rangle\mu(k)/2 \tag{17}$$

for *all* states $|\psi_f\rangle$. These operators yield a system described by $|\psi_i\rangle$ in complete equilibrium with the solvent. These yield for ΔE_{qm}

$$\Delta E_{qm,A} = \langle\Psi_f|H^0|\Psi_f\rangle - \langle\Psi_i|H^0|\Psi_i\rangle - g(\varepsilon)\langle\psi_i|\mu|\psi_i\rangle\cdot(\langle\psi_f|\mu|\psi_f\rangle - \langle\psi_i|\mu|\psi_i\rangle) \tag{18}$$

and

$$\Delta E_{qm,B} = \langle\Psi_f|H^0|\Psi_f\rangle - \langle\Psi_i|H^0|\Psi_i\rangle - g(\varepsilon)\langle\psi_i|\mu|\psi_i\rangle\cdot(\langle\psi_f|\mu|\psi_f\rangle - \langle\psi_i|\mu|\psi_i\rangle)/2, \tag{19}$$

respectively, to which corrections must be added to yield Eq. (6). Simply adding the terms without correcting the wave function (i.e., using the wavefunction from Eqs. (16) or (17)) is equivalent to first-order perturbation theory. One of the important goals of this paper is to numerically check the accuracy of this much simpler and much faster "first-order" approximation, at least for absorption spectra. For

Table 1. Comparison of calculated geometries with the crystallographic geometry

Bond lengths (Å)	Ground state				INDO/1 ROHF exc. 0°	INDO/1 ROHF exc. 90°
	HF STO-3G (Ref. [21])	CASSCF (Ref. [8])	INDO/1	Exp. (Ref. [20])		
N1–C2	1.157	1.157	1.200	1.145	1.214	1.288
C2–C3	1.458	1.446	1.424	1.434	1.387	1.449
C3–C4	1.394	1.399	1.402	1.388	1.451	1.451
C4–C5	1.379	1.391	1.389	1.370	1.354	1.433
C5–C6	1.402	1.406	1.407	1.400	1.447	1.462
C6–N7	1.446	1.388	1.399	1.367	1.387	1.426
N7–C8	1.486	1.460	1.422	1.456	1.422	1.434
Angles (degrees)						
C3–C4–C5	120.8	120.0	121.0	–	120.5	120.5
C4–C5–C6	121.1	121.4	120.2	–	120.8	120.9
C5–C6–N7	121.5	121.3	120.5	–	120.6	120.8
C6–C7–C8	122.4	122.2	120.1	121.6	121.0	119.1
C8–N7–C8′	115.1	115.6	119.8	116.4	118.1	121.8
Dihedral angles (degrees)						
C5–C6–N7–C8	41.8	21.2	0.0	11.9	0.0	0.0

emission we would need to replace $|\psi_i\rangle$ in Eqs. (16) and (17) with $|\psi_f\rangle$ and *attempt* the SCF problem for an excited state. This is often not successful.

2. Calculational details

All calculations have been performed with the ZINDO program package [17]. The geometry optimization of DMABN and CBQ have been done with the INDO/1 Hamiltonian [18]. The geometry of DMABN was optimized with the C_{2v} symmetry restriction. When the C_{2v} symmetry restriction is used in the geometry optimization, both a planar excited state and a twisted excited state can be obtained. However, we force the dimethylamino group to be planar with this choice of symmetry. An optimization of the ground state of DMABN without symmetry restrictions was also performed to estimate the size of the error we introduce by restricting the geometry to C_{2v} symmetry. The geometry we obtained from the latter optimization agrees very well with the C_{2v} symmetry geometry and the dimethylamino group remained planar. The INDO/1 geometry is compared with experimental geometries and other calculated geometries in Table 1. The geometry of the ground state and the first excited state of CBQ was also obtained from a INDO/1 optimization. No symmetry constraints were used when the CBQ geometry was optimized. The excited state geometries of both DMABN and CBQ were obtained using a singlet restricted open-shell Hartree–Fock (ROHF) approach.

All spectra were calculated with the INDO/S Hamiltonian. All possible single excitations from all occupied orbits of π type and lone-pair type to all virtual π^* type and lone-pair* type orbitals were included in the spectra calculations of DMABN. With this selection of the CI space a total of 257 configurations were

included in the CI calculation. The CI space for CBQ was obtained in a similar way and a total of 232 configurations was included in the spectral calculations on CBQ.

In this work we have used a spherical solvent cavity. The cavity radius is obtained from the mass density formula [1] and is 3.87 Å for DMABN and 4.18 Å for CBQ. With this selection of cavity, the molecules are completely enclosed in the solvent free sphere.

3. Results and discussion

In Table 2, the calculated absorption spectra of DMABN, in different solvents, are compared with experimental absorption spectra. The character of the two first excited states is not changed by the solvent, however, the relative order of the states is sometimes shifted. The 1^1A to 2^1A transition is the most intense and is due to a $\pi \rightarrow \pi^*$ transition (91% HOMO to LUMO). The transition moment is along the molecular axis, from the benzonitrile group to the dimethylamino group. The second transition is also a $\pi \rightarrow \pi^*$ transition (22% HOMO-1 to LUMO and 76% HOMO to LUMO + 1). The transition moment is perpendicular to the first transition moment and is in the benzonitrile plane. The first-order SCRF results are very close to the results obtained with the fully relaxed theory no matter which model we use. The largest difference between the calculated absorption energies, using the two SCRF formulations, is 600 cm^{-1} (0.07 eV). The mean difference between calculated absorption energies using the two SCRF theories are for the ^1B state, 183 cm^{-1} (0.02 eV), and for the ^1A state, 100 cm^{-1} (0.01 eV). The largest difference of the predicted absorption energies using the two approaches is found for the ^1B state in pyridine solution using model B.

All four methods in both SCRF formulations give reasonable absorption energies compared to the experimental numbers. The largest deviation from the experimental energies is found for models A and B. However, the predicted absorption energies are off at most by 2900 cm^{-1} (0.35 eV) for the ^1B state in cyclohexane solution (A(full) method). The mean deviation from experimental energies for the SCRF [1] theory is 1525 cm^{-1} (0.19 eV) and for the SCRF (full) theory is the mean deviation is 1675 cm^{-1} (0.21 eV). All absorption energies are calculated too low compared to the experimental energies. Thus, the solvent shift is slightly overestimated. This can be due to too small a solvent radius, or to the fact that the INDO/1 optimization predicts the dimethylamino group to be the planar.

One test calculation with the INDO/1 geometry and with the experimental wagging angle of the dimethylamino group (12°) was performed. The wagging vibrational mode of the dimethylamino group corresponds to a change in hybridization of the nitrogen atom from sp^2 to sp^3. The predicted energies were shifted up to higher energies by 1600 cm^{-1} for the ^1B state and 900 cm^{-1} for the ^1A state (method A(1), acetonitrile). Furthermore, a small decrease in dipole moment was observed. These observations argue against the N-inversion mechanism for the dual fluorescence of DMABN proposed by Zachariasse et al. [7, 23]. However, to be consistent we kept the INDO/1 geometry in all further calculations.

The predicted absorption spectra of CBQ in methanol is compared with experimental spectra in Table 3.

The positions of the absorption maximum of CBQ are almost solvent independent. Thus, we have just calculated the absorption spectrum in one solvent. The small solvent shift is due to the small change in the charge distribution upon

Table 2. A comparison between the calculated absorption spectra of DMABN, in different solvents, with experimental spectra. Two different formulations of the self-consistent reaction field method have been used. The experimental absorption energies are taken from Ref. [22] and references therein and the experimental excited state dipole moment is from Ref. [23]. Kk = kilo-Kraisers = 1000 cm^{-1}

Method	Excited state						Experimental			
	^1A			^1B			^1A		^1B	
	Energy (kK)	f_{osc}	μ (D)	Energy (kK)	f_{osc}	μ (D)	Energy (kK)	μ (D)	Energy (kK)	μ (D)
Cyclohexane										
A(1)	33.1	0.62	14.8	33.2	0.03	10.5	35.5	17.0	33.1	9.9
A(full)	33.0	0.64	16.2	33.2	0.03	10.8				
B(1)	33.2	0.61	13.4	33.1	0.03	9.4				
B(full)	33.0	0.64	16.2	33.2	0.03	10.9				
A1(1)	34.4	0.63	14.8	33.5	0.03	10.5				
A1(full)	34.4	0.62	14.0	33.5	0.03	9.5				
B1(1)	34.4	0.61	13.4	33.4	0.03	9.4				
B1(full)	34.4	0.62	13.9	33.5	0.03	9.5				
Pyridine										
A(1)	31.1	0.67	19.4	32.6	0.04	14.6	33.9		n.o.	
A(full)	31.0	0.72	22.2	32.7	0.04	15.7				
B(1)	31.6	0.63	15.1	32.7	0.03	10.7				
B(full)	31.0	0.67	19.1	32.6	0.04	13.1				
A1(1)	33.6	0.67	19.4	33.6	0.04	14.6				
A1(full)	33.3	0.65	17.8	33.3	0.04	12.5				
B1(1)	33.2	0.63	15.1	33.1	0.03	10.7				
B1(full)	33.2	0.64	15.9	33.0	0.03	11.3				
Acetonitrile										
A(1)	31.5	0.69	20.5	32.8	0.04	15.6	33.9		n.o.	
A(full)	31.7	0.73	22.9	32.9	0.04	16.7				
B(1)	31.9	0.63	15.4	32.7	0.03	10.9				
B(full)	31.5	0.66	18.4	32.7	0.04	12.8				
A1(1)	33.7	0.69	20.5	33.7	0.04	15.6				
A1(full)	33.4	0.67	19.0	33.4	0.04	13.8				
B1(1)	33.2	0.63	15.4	33.1	0.03	10.9				
B1(full)	33.2	0.64	16.0	33.1	0.03	11.1				

Table 3. The experimental absorption spectrum is compared with calculated absorption spectra of CBQ in methanol solution. The experimental spectrum is taken from Ref. [23]

Method	First strong band			Second strong band			Experimental			
	Energy (kK)	f_{osc}	μ (D)	Energy (kK)	f_{osc}	μ (D)	Energy (kK)	ε_{mol}	Energy (kK)	ε_{mol}
Methanol										
A(1)	36.9	0.30	11.6	43.6	0.24	9.7	35.9	3000	42.8	4000
A(full)	37.0	0.29	12.1	43.6	0.25	9.9				
B(1)	37.0	0.30	9.3	43.7	0.22	7.8				
B(full)	36.9	0.31	10.4	43.6	0.23	8.7				
A1(1)	37.3	0.30	11.6	43.8	0.24	9.7				
A1(full)	37.3	0.30	10.8	43.8	0.23	9.0				
B1(1)	37.3	0.31	9.3	43.8	0.22	7.8				
B1(full)	37.3	0.31	9.5	43.8	0.22	7.9				

excitation. In the region of 31 000–3700 cm^{-1} three weak peaks appear but the strong peak at 37 000 cm^{-1} overlaps these transitions. The first weak transition corresponds to a charge transfer from the amino group to the benzonitrile group. Thus, the transition moment is polarized along the molecular axis. The first two band maxima have $\pi \rightarrow \pi^*$ character and the transitions are more localized to the benzonitrile group. All four methods give good agreement with the experimental results and the two formulations of the SCRF theory give almost identical results.

The above results give us confidence to apply the fully relaxed theory to the emission problem. The potential energy surfaces of the ground state and the first two excited states of DMABN, when the dimethylamino group is twisted, are depicted in Fig. 4. All states are fully relaxed with respect to the solvent electrons and the solvent nucleus. Thus, these are the potential energy surfaces for emission. In the gas phase we predict a small barrier for the twisting of the ^1A state (2.9 kcal/mol); in cyclohexane the barrier is only 0.6 kcal/mol and in the two polar solvents the barrier vanishes. The INDO method is not expected to give that good an accuracy that these numbers can be used with great confidence. However, the trend is in good agreement with the observed facts that in non-polar solvents the fluorescence spectrum has only one peak (B*), and in polar solvents two peaks.

The predicted fluorescence spectra of DMABN are summarized in Table 4. The experimental fluorescence spectrum of DMABN in nonpolar solvents has just one peak but the band shape is unsymmetrical with a broader tail towards lower energies. Schuddeboom et al. resolved the tail of the emission band in cyclohexane solution by subtracting the fluorescence spectrum of 4-(methylamino)benzonitrile [23]. In polar solvents of medium dielectric strength, two separate bands can be observed and in very polar solvents the A* band dominates and the B* band is observed as a shoulder on the very broad A* band. Furthermore, the lifetime of the B* state is very small, in the picosecond region, while the lifetime of the A* state is in the nanosecond region [23]. The calculated oscillator strengths for the emission compare well with this picture. The oscillator strength is proportional to the inverse of the lifetime. All the experimental fluorescence energies correspond to the band maximum of each peak. In the fully twisted conformer the transition is completely forbidden and emission would take place more readily from a vibrational excited state ("hot fluorescence").

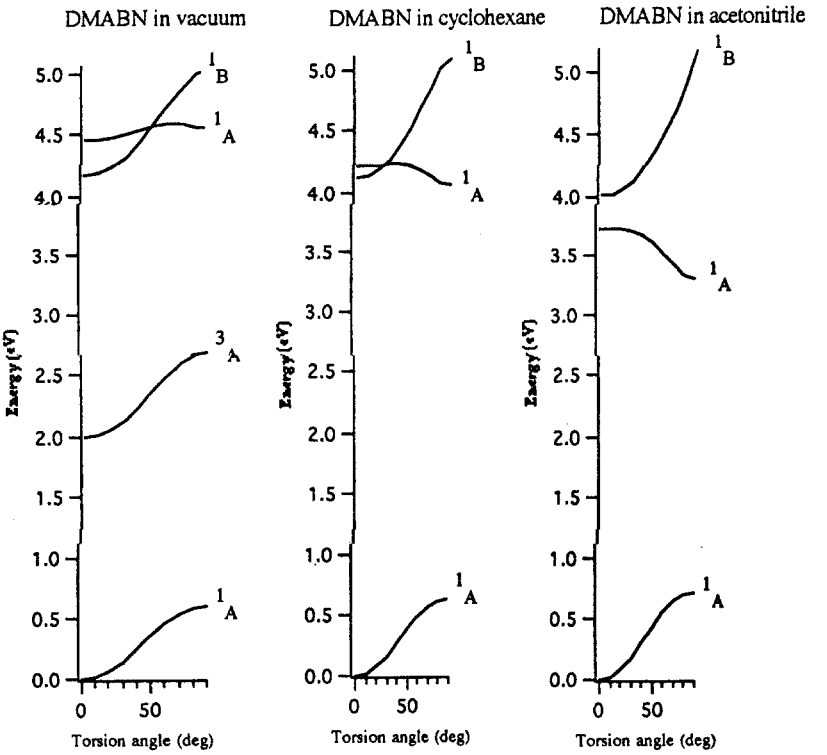

Fig. 4. Potential energy "emission" surfaces for DMABN in gas phase and two different solvents

Table 4. Comparison of calculated and experimental fluorescence spectra of DMABN. Experimental number from Ref [22] and references therein, and from Ref. [23]

Method	Planar (B*)		Twisted (A*)		Experimental	
	Energy (kK)	f_{osc}	Energy (kK)	f_{osc}	Energy B* (kK)	Energy A* (kK)
Cyclohexane						
A(full)	30.6	0.75	22.9	0.00	29.0	26.0
B(full)	30.6	0.75	22.9	0.00		
A1(full)	31.6	0.73	25.8	0.00		
B1(full)	31.6	0.73	25.8	0.00		
Pyridine						
A(full)	28.5	0.98	12.5	0.00	27.4	22.6
B(full)	28.4	0.83	15.6	0.00		
A1(full)	30.2	0.83	20.1	0.00		
B1(full)	30.1	0.76	20.9	0.00		
Acetonitrile						
A(full)	28.8	1.10	9.8	0.00	27.4	21.0
B(full)	28.4	0.83	15.6	0.00		
A1(full)	30.1	0.92	17.7	0.00		
B1(full)	29.7	0.77	19.4	0.00		

Table 5. Comparison between calculated and experimental fluorescence spectrum of CBQ in different solvents

Method	Calculated		Experimental energy (kK)
	Energy (kK)	f_{osc} ($\times 10^4$)	
Isooctane			
A(full)	27.2	1.0	25.3
B(full)	27.2	1.0	
A1(full)	29.1	2.0	
B1(full)	29.1	2.0	
Methanol			
A(full)	21.1	2.0	21.3
B(full)	22.4	1.0	
A1(ful)	24.4	1.0	
B1(full)	24.7	1.0	

The question then is whether the calculated energies for the A* fluorescence should be compared with the band maximum or with the low energy limit of the A* band.

From the potential energy surfaces in Fig. 4 we can conclude that the fully twisted conformer corresponds to a local energy minimum and every vibration along the twisting coordinate will increase the calculated fluorescence energy. Thus we conclude that the energies we calculated for the A* band are the low energy limit. With the above interpretation of the calculated fluorescence spectra the agreement between the calculated spectra and the experimental spectra is acceptable, with an exception for model A.

The geometry of the amino group of CBQ corresponds to the twisted conformer of DMABN with a wagging angle of about 30°. The experimental fluorescence spectrum of CBQ has only one band and the position of the band corresponds to the position of the A* band in DMABN. This was taken as a proof for the TICT mechanism of the dual fluorescence but both the twisting and the wagging effect are included in the CBQ geometry. The calculated spectra of CBQ are compared with experimental spectra in Table 5. The calculated energies for the fluorescence should correspond to the observed band maximum tabulated in Table 5. The calculated fluorescence spectra agree well with the experimental spectra.

Model A gives much too large a shift, especially in acetonitrile. If we assume that the calculated energy for the A* fluorescence should be compared with the low energy limit of the experimental spectra, the best agreement between theory and experiment is obtained using model B.

4. Summary

We have presented a self-consistent reaction field theory that can be used to calculate both absorption and emission spectra in solution. The solute, or perhaps

the solute with several specifically bound solvent molecules treated as a supermolecule, are treated quantum mechanically in a solvent that is treated as a continuum. The SCRF theory outlined here accounts for full electronic relaxation of the solvent electrons. The results from the fully relaxed SCRF theory compares very well with the results from a SCRF theory in which the solvent electrons are allowed to relax only through first order in perturbation theory.

Both formulations of the SCRF theory give good agreement between calculated absorption spectra and experimental spectra. The emission spectra of the two test molecules reported here, as well as others, are reasonably well reproduced.

Our calculations support the TICT mechanism for the dual fluorescence of DMABN and the wagging vibrational activation suggested by Zachariasse et al. [7] seems to be less important. This conclusion was also reached by Serrano-Andres et al. [8] based upon CASSCF/CASPT2 (gas phase) calculations.

Acknowledgments. This manuscript is dedicated to Professor Jan Linderberg, a good friend, and a model for all of us when it comes to practicing our trade. Jan is careful and still wildly creative. He once said that he went to bed with tables of integrals, because it was great fun – that all integrals are interesting. Jan's interests scan everything, from exact to approximate models of quantum chemistry, and all aspects of dynamics, and he has made important contributions in all these areas. We hope that he will enjoy this "model" of solvation. As simple as it is, it seems to capture the essential physics of the situation.

The Swedish Natural Science Research Council (NFR), the office of Naval Research Office (US) and the National Science Foundation CHE 9441940 are acknowledged for financial support. Professor Björn Roos and coworkers are acknowledged for giving us a preprint of their related work on DMABN.

References

1. Karelson MM, Zerner MC (1992) J Phys Chem 96:6950.
2. (a) Broo A, Larsson S (1992) Chem Phys 161:363; (b) Broo A, (1993) Chem Phys 169:131; (c) Broo A (1994) in press Chem Phys 182:000.
3. Lippert E, Lüder W, Moll F, Nagele W, Boos H, Prigge H, Seibold-Blankenstein I (1961) Angew Chem 73:695; Lippert E, Lüder W, Boos H (1962) In Vol 3, p 183 Advances in molecular spectroscopy, Pergamon Press, Oxford, pp. 443.
4. Khalil OS, Hofeldt RH, McGlynn SP (1972) Chem Phys Letters 17:479.
5. Rotkiewicz K, Grellmann KH, Grabowski ZR (1973) Chem Phys Letters 19:315; (1973) 21:212.
6. Rettig W (1986) Angew Chem Int Ed Engl 25:971; Kavarnos GJ (1993) Fundamentals of photoinduced electron transfer. VCH Publishers, New York, pp 196.
7. Leinhos U, Kühnle W, Zachariasse KA (1991) J Phys Chem 95:2013; Zachariasse KA, von der Haar T, Bebecker H, Leinhos U, Kühnle W (1993) Pure Appl Chem 65:1745.
8. Serrano-Andres L, Merchan M, Roos BO, Lindh R to be published.
9. Rotkiewicz K, Rubaszewska W (1980) Chem Phys Letters 70:444.
10. Tapia O, Goscinski O (1975) Mol Phys 29:1653; Tapia O (1983) In Ratajcjak H, Orville-Thomas WJ (eds) Interactions, Wiley, Chichester.
11. Thole BT, Th van Duijnen P (1980) Theoret Chim Acta 55:307; Miertun S, Scrocco E, Tomasi J (1981) Chem Phys 55:17.
12. Rivail J-L, Rinaldi D (1976) Chem Phys 18:233; Rivail J-L, Terryn B (1982) J Chem Phys 79:1.
13. Kirkwood JG (1934) J Chem Phys 7:351.
14. Onsager L (1936) J Am Chem Soc 58:1486.
15. Mikkelsen KV, Ågren H, Jensen H-JA, Helgaker T (1988) J Chem Phys 89:3086.
16. Zheng X, Zerner MC (1993) Intern J Quantum Chem Symp 27:431.
17. ZINDO Program package: M.C. Zerner University of Florida, Gainesville.
18. Bacon AD, Zerner MC (1979) Theoret Chim Acta 53:21; Pople JA, Beveridge DA, Dobosch PA (1967) J Phys Chem 47:2026.

19. Ridley JE, Zerner MC (1973) Theoret Chim Acta 32:111; Zerner MC, Loew GH, Kirschner RF, Mueller-Westerhoff UT (1980) J Am Chem Soc 102:589.
20. Heine A, Herbst-Irmer R, Stalke D, Kühnle W, Zachariasse KA (1994) Acta Cryst B50, in press.
21. Kato S, Amatatsu Y (1990) J Chem Phys 92:7241.
22. Lipinski J, Chojnacki H, Grabowski ZR, Rotkiewicz K (1980) Chem Phys Letters 70:449.
23. Schuddeboom W, Jonker SA, Warman JM, Leinhos U, Kühnle W, Zachariasse KA (1992) J Phys Chem 96:10809.